AGU PUBLICATIONS

Water Resources Research

RESEARCH ARTICLE
10.1002/2016WR019625

Replenishing an unconfined coastal aquifer to control seawater intrusion: Injection or infiltration?

Chunhui Lu[1], Wenlong Shi[1], Pei Xin[1], Jichun Wu[2], and Adrian D. Werner[3,4]

[1]State Key Laboratory of Hydrology-Water Resources and Hydraulic Engineering, Hohai University, Nanjing, China, [2]Key Laboratory of Surficial Geochemistry, Ministry of Education, Department of Hydrosciences, School of Earth Sciences and Engineering, Nanjing University, Nanjing, China, [3]National Centre for Groundwater Research and Training, Flinders University, Adelaide, South Australia, Australia, [4]School of the Environment, Flinders University, Adelaide, South Australia, Australia

Key Points:
- The performance of a circular pond is the same as that of an injection well
- A method is introduced to derive the maximum net extraction
- The maximum net extraction rate depends on the pond shape

Correspondence to:
C. Lu,
chunhui.hohai@outlook.com

Citation:
Lu, C., W. Shi, P. Xin, J. Wu, and A. D. Werner (2017), Replenishing an unconfined coastal aquifer to control seawater intrusion: Injection or infiltration?, *Water Resour. Res.*, *53*, 4775–4786, doi:10.1002/2016WR019625.

Received 9 AUG 2016
Accepted 14 MAY 2017
Accepted article online 19 MAY 2017
Published online 9 JUN 2017

Abstract In this study, we compare the performances of well injection and pond infiltration in controlling seawater intrusion in an unconfined coastal aquifer through two scenario groups: (1) a single injection well versus an elliptic infiltration pond and (2) an injection-extraction well pair system versus an elliptic infiltration pond-extraction well system. Comparison is based on quantitative indicators that include the interface toe location, saltwater volume, and maximum net extraction rate (for scenario 2). We introduce a method to determine the maximum net extraction rate for cases where the locations of stagnation points cannot be easily derived. Analytical analysis shows that the performances of injection and infiltration are the same, provided that the pond shape is circular. The examination of scenario group 1 suggests that the shape of the infiltration pond has a minor effect on the interface toe location as well as the reduction in the saltwater volume, given the same total recharge rate. The investigation of scenario group 2 indicates, by contrast, that the maximum net extraction rate increases significantly with the increasing ratio of b to a, where a and b are semiaxes of the ellipse parallel and perpendicular to the coastline, respectively. Specifically, for a typical aquifer assumed, an increase of 40% is obtained for the maximum net extraction when b/a increases from 1/200 to 200. Despite that the study is based on a simplified model, the results provide initial guidance for practitioners when planning to use an aquifer recharge strategy to restore a salinized unconfined coastal aquifer.

1. Introduction

Groundwater stored in coastal aquifers provides water supplies for a variety of purposes. Excessive groundwater withdrawals have caused encroachment of seawater into the fresh regions of coastal aquifers, resulting in a worldwide seawater intrusion problem [*Werner et al.*, 2013]. Regional and global climate change, such as extreme/extended drought events and sea-level rise due to global warming, exacerbates the problem further [*Werner and Simmons*, 2009; *Ataie-Ashtiani et al.*, 2013; *Lu et al.*, 2013a, 2013b, 2015]. Seawater intrusion into coastal aquifers could cause serious consequences in terms of both environmental and economic impacts, for which effective management strategies are required [e.g., *Werner*, 2010; *Shi and Jiao*, 2014].

To protect the freshwater within coastal aquifers from being contaminated by salt water, various strategies have been proposed in the past decades. The appropriate design of well fields (including locations and extraction rates) is the most pragmatic and cost-effective measure for preventing seawater intrusion [*Strack*, 1976]. This idea has led to the development of pumping optimization strategies for multiple-well systems [e.g., *Cheng et al.*, 2000; *Mantoglou*, 2003; *Ataie-Ashtiani and Ketabchi*, 2011]. These methods seek critical well locations and/or pumping rates to minimize the extent of seawater intrusion and/or optimize pumping rates. In some cases, freshwater pumped from skimming wells (especially from thick aquifers) has been found to minimize drawdown and maximize allowable extraction rates, thereby avoiding aquifer salinization in the most cost-effective manner [*Saeed*, 2002].

Other methods of avoiding and mitigating seawater intrusion include the introduction of subsurface barriers, using a variety of configurations [e.g., *Sheahan*, 1977; *Mahesha*, 1996, 2001; *Rao et al.*, 2004; *Strack et al.*, 2016]. Given that the interface toe moves significantly faster during seawater retreat than during

seawater intrusion (for symmetric water level changes [*Chang and Clement*, 2012; *Lu and Werner*, 2013]), simply replenishing the aquifer may be effective in mitigating seawater intrusion. Alternatively, artificial recharge has been widely adopted in practice to create hydraulic barriers capable of preventing seawater from moving inland [e.g., *Luyun et al*., 2011; *Herndon and Markus*, 2014]. There are many examples of the successful application of this strategy in the US, including the West Coast Barrier, the Dominguez Gap Barrier, and the Alamitos Gap Barrier installed at the Los Angeles County and the Orange County in California [*Land et al*., 2004].

The performance of hydraulic barriers in preventing seawater intrusion has been investigated analytically by comparing the maximum pumping rate of a single extraction well with the maximum net extraction rate of an injection-extraction well pair (a proportion of extracted fresh groundwater is reinjected through the injection well located between the interface toe and extraction well) [*Lu et al*., 2013a, 2013b]. The injection-extraction well pair system significantly outperforms a traditional single extraction well in terms of the net extraction rate for a broad range of well placement and pumping rates, highlighting the potential benefit of developing a hydraulic barrier in controlling seawater intrusion. Similar to the well pair introduced by *Lu et al*. [2013b], a hydrothermal doublet was recently introduced by *Keuleneer and Renard* [2015] with the combined aim of seawater intrusion remediation and energy production.

Apart from developing positive hydraulic barriers (i.e., recharging freshwater into an aquifer), negative hydraulic barriers (i.e., extraction of salt water) have been considered as a means of intercepting inflowing saltwater [*Verruijt*, 1969; *Todd*, 1980; *Sherif and Hamza*, 2001; *Kacimov et al*., 2009; *Masciopinto*, 2013]. The main disadvantage of this scheme is that it often leads to a significant loss of fresh groundwater resources, because the well inevitably pumps freshwater after a period of time. To minimize this drawback, *Pool and Carrera* [2010] proposed a double pumping barrier system: an inland well extracts freshwater and a seaward well extracts salt water. The results of numerical modeling by *Pool and Carrera* [2010] indicated that the proposed system outperforms a single-well negative barrier.

In addition to hydraulic barriers, solid and gaseous barriers have been reported to block or retard seawater intrusion. The solid barriers adopting low-permeability subsurface walls (e.g., slurry, gypsum, steel, or concrete) to reduce the extent of salt water in coastal aquifers are often applicable only in shallow aquifers [*Sugio et al*., 1987; *Luyun et al*., 2009; *Kaleris and Ziogas*, 2013; *Strack et al*., 2016]. Besides, considerable engineering and investment are required for constructing solid barrier systems, and hence they are often considered inefficient in terms of costs [*Pool and Carrera*, 2010]. Using gas injection to mitigate aquifer salinization by reducing the hydraulic conductivity of aquifer media has been considered cost-effective, in comparison with potable-water injection [*Sun and Semprich*, 2013]. However, the successful implementation of this technology is a challenging and multidisciplinary task, which requires further investigation.

Among the strategies reported, artificial recharge through either well injection or pond infiltration is adopted most commonly in practice to remediate salinized unconfined coastal aquifers [*Raicy et al*., 2012; *Eslamian*, 2014]. In practice, both injectant and infiltration are sourced from diverted surface water, which could be a combination of natural runoff, regulated releases from reservoirs, imported water, and reclaimed sewage effluent [*Lee and Normark*, 2009]. To the best of our knowledge, however, the relative performances of well injection and pond infiltration in remediating seawater intrusion have not been compared. Investigation is urgently required to fill this knowledge gap to guide aquifer recharge strategies aimed at restoring salinized unconfined coastal aquifers.

This study aims to compare the performances of well injection and pond infiltration in controlling seawater intrusion in unconfined coastal aquifers. Two scenario groups will be considered. First, a single injection well is compared with an elliptic infiltration pond by quantifying their performances in causing both the interface toe to retreat and the saltwater volume to reduce. The importance of quantifying the saltwater volume has been highlighted by *Werner et al*. [2012] and *Lu et al*. [2013a]. Second, an injection-extraction well pair system is compared with an elliptic infiltration pond-extraction well system by quantifying the maximum net extraction rate achievable from each. Quantitative indicators, including the interface toe location, saltwater volume, and maximum net extraction rate, are derived to perform the comparison.

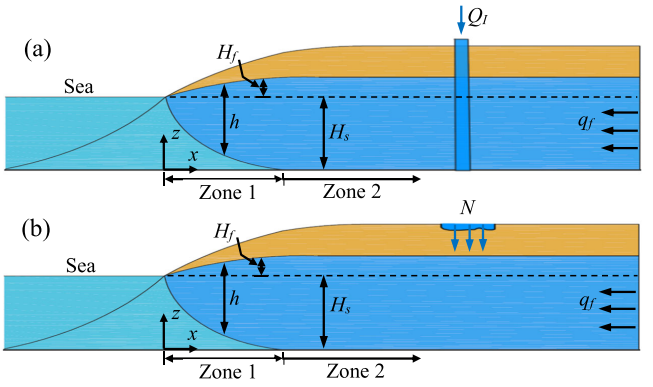

Figure 1. The cross section of an unconfined, isotropic, homogenous coastal aquifer with an (a) injection well and (b) infiltration pond.

2. Conceptual Model

We consider an idealized unconfined coastal aquifer, which is horizontal, isotropic, and homogenous with a constant inflow rate of q_f [L^2T^{-1}] (negative) from inland. The cross section of the aquifer is shown in Figure 1. The aquifer is assumed infinite in the y direction and semi-infinite in the x direction. The y axis is aligned with the coastline, while the x axis points inland. The elevation of mean sea level above the confining bed is H_s [L], and the elevation of the water table above mean sea level is H_f [L]. We denote the thickness of the freshwater lens as h [L]. As shown, a saltwater wedge is developed to reach an equilibrium (steady state) condition. Zones 1 and 2 in the figure represent, respectively, an interface zone and a freshwater zone.

Two scenario groups are considered for comparison. First, an injection well (Figure 1a) is compared with an infiltration pond (Figure 1b). The extraction well is located at a distance of L_I [L] from the coastline, with an injection rate of Q_I [L^3T^{-1}] distributed uniformly throughout the saturated thickness of the aquifer. The infiltration pond is assumed elliptic in shape with the center at a distance of L_I [L] from the coastline (i.e., the same as the location of the injection well), and the axes of the ellipse along the x axis and y axis are a and b (see Figure 2), respectively. The pond has an infiltration rate of N [LT^{-1}] and an area of $A = \pi ab$ [L^2]. To facilitate the comparison of the effectiveness of well injection and pond infiltration, $Q_I = NA$ is assumed, i.e., the two recharge schemes have equal total recharge rates. Second, an injection-extraction well pair system, as introduced by *Lu et al*. [2013b], is compared with an infiltration pond-extraction well system. The assumptions in the first scenario group are also adopted in the second scenario group. The location of the extraction well is the same in the two systems and at a distance of L_E [L] ($L_E > L_I$) from the coastline. Q_E [L^3T^{-1}] is the extraction rate, and Q_N [L^3T^{-1}] ($=Q_E - Q_I$) is the net extraction rate in the injection-extraction and infiltration-extraction systems. The maximum allowable extraction rate is sought that precludes the interception of salt water by the extraction well.

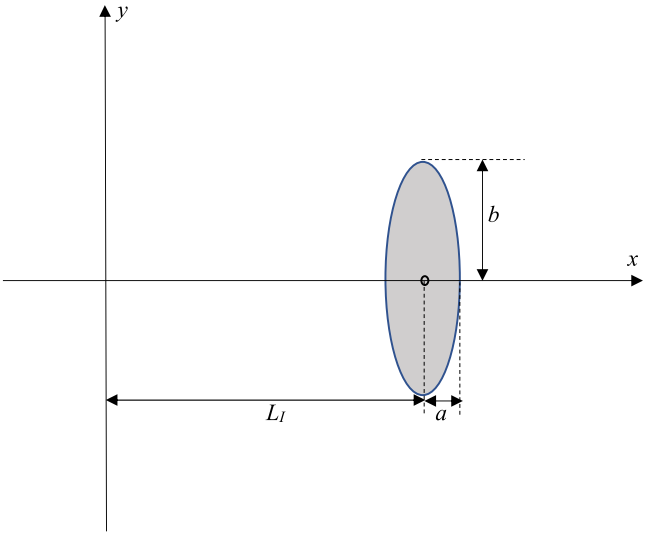

Figure 2. Plan view of an elliptic infiltration pond.

3. Mathematical Derivation

3.1. Interface Toe Location and Saltwater Volume of the First Scenario Group

Following *Strack*'s [1976] potential theory for interface problems, we derive the interface toe location in terms of the x coordinate of the interface at $z = 0$ for the two aquifer recharge schemes. The theory is based on several assumptions: (1) the mixing between freshwater and seawater is neglected and an interface exists; (2) the sea level is constant and the system is under steady state; (3) the Dupuit-Forchheimer approximation is adopted such that the resistance to flow in the vertical direction is neglected; and (4) the Ghyben-Herzberg relation is

applicable for determining the interface toe location. In addition, when the flow system involves infiltration/injection and extraction, it is assumed that aquifer recharge would not lead to land surface seepage and extraction would not result in a dry aquifer, despite that these factors must be considered for real cases.

A discharge potential, Φ [L^3T^{-1}], can be defined for Zones 1 and 2, respectively [*Strack*, 1976],

$$\text{Zone1}: \Phi=\frac{(1+\alpha)}{2\alpha}K(\phi-H_s)^2+\frac{(1+\alpha)}{2}KH_s^2, \tag{1a}$$

$$\text{Zone2}: \Phi=\frac{1}{2}K\phi^2, \tag{1b}$$

where K [LT^{-1}] is the hydraulic conductivity of the aquifer, α is the density ratio defined as the density difference between seawater and freshwater relative to the freshwater density, usually adopting a value of 0.025, and ϕ [L] is the head, expressed by $\frac{\alpha}{(1+\alpha)}h+H_s$ and h for Zones 1 and 2, respectively. The potential at the interface toe is then derived by letting $\phi=(1+\alpha)H_s$ [*Strack*, 1976],

$$\Phi_t=\frac{(1+\alpha)^2}{2}KH_s^2. \tag{2}$$

When the flow field is developed by regional flow in the direction of a constant-head water body (i.e., the sea), superimposed by an injection well or an elliptic infiltration pond, the discharge potential can be expressed respectively as [*Strack*, 1989; *Strack*, 2009],

$$\text{Well injection}: \Phi_W=-q_fx+\frac{Q_I}{4\pi}\ln\left[\frac{(x+L_I)^2+y^2}{(x-L_I)^2+y^2}\right]+\frac{(1+\alpha)}{2}KH_s^2, \tag{3}$$

$$\text{Elliptic pond infiltration}: \Phi_P=-q_fx-G+\Re(\Omega_2)+\frac{(1+\alpha)}{2}KH_s^2, \tag{4}$$

in which $\Re$ represents the real part of the function, and G is a function described by

$$G=\frac{Q_I}{4\pi ab(a+b)}\left[2b(x-L_I)^2+2ay^2-ab(a+b)\right] \text{ for } \left(\frac{x-L_I}{a}\right)^2+\left(\frac{y}{b}\right)^2\le 1, \tag{5a}$$

$$G=\Re(\Omega_1) \text{ for } \left(\frac{x-L_I}{a}\right)^2+\left(\frac{y}{b}\right)^2>1. \tag{5b}$$

Ω_1 and Ω_2 are complex potentials expressed in Appendix A. Note that inside the recharge area, the discharge potential is governed by the Poisson equation (i.e., $\nabla^2\Phi_P=-N$), and outside the recharge area, the Laplace equation (i.e., $\nabla^2\Phi_P=0$). Figure 3 shows the contour lines of the discharge potential of elliptic pond infiltration (i.e., based on equation (4)), where $b/a=10$ and 1/10 are selected. It is clearly shown that the equipotentials are in a close-up around the pond boundary and also continuous in value and slope. When the infiltration pond is circular, the discharge potential is written as [*Strack*, 1989; *Lu et al.*, 2009],

$$\Phi_P=-q_fx-H+\frac{Q_I}{4\pi}\ln\left[\frac{(x+L_I)^2+y^2}{a^2}\right]+\frac{(1+\alpha)}{2}KH_s^2, \tag{6}$$

in which H is a function described by

$$H=\frac{Q_I}{4\pi a^2}\left[(x-L_I)^2+y^2-a^2\right] \text{ for } (x-L_I)^2+y^2\le a^2, \tag{7a}$$

$$H=\frac{Q_I}{4\pi}\ln\left[\frac{(x-L_I)^2+y^2}{a^2}\right] \text{ for } (x-L_I)^2+y^2>a^2 \tag{7b}$$

The location of the interface toe $(x, y)=(x_t, y_t)$ can be found for the two schemes by combining equations (2) and (3) (letting $\Phi_W=\Phi_t$), and equations (2) and (4) or (6) (letting $\Phi_P=\Phi_t$), respectively,

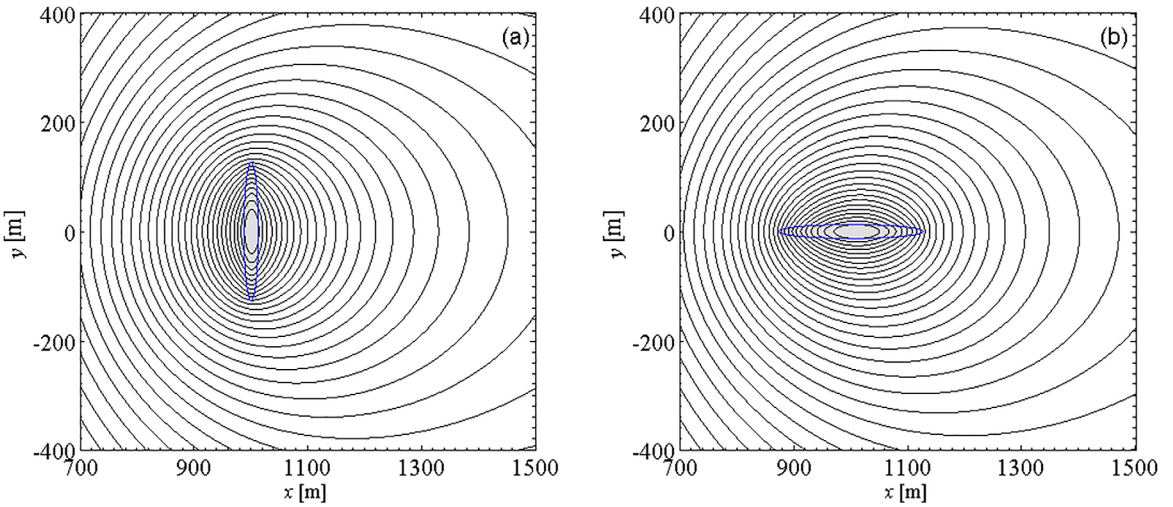

Figure 3. The contour lines of the discharge potential in the case of an elliptic infiltration pond (gray area): (a) $b/a = 10$ and (b) $b/a = 1/10$.

$$\text{Well injection}: \frac{(1+\alpha)^2}{2}KH_s^2 = -q_f x + \frac{Q_I}{4\pi}\ln\left[\frac{(x+L_I)^2+y^2}{(x-L_I)^2+y^2}\right] + \frac{(1+\alpha)}{2}KH_s^2, \tag{8}$$

$$\text{Elliptic pond infiltration}: \frac{(1+\alpha)^2}{2}KH_s^2 = -q_f x - G + \Re(\Omega_2) + \frac{(1+\alpha)}{2}KH_s^2, \tag{9}$$

$$\text{Circular pond infiltration}: \frac{(1+\alpha)^2}{2}KH_s^2 = -q_f x - H + \frac{Q_I}{4\pi}\ln\left[\frac{(x+L_I)^2+y^2}{a^2}\right] + \frac{(1+\alpha)}{2}KH_s^2. \tag{10}$$

Equations (8–10) can be solved using the Newton-Raphson method. Note that the initial interface toe location (x_i) in the absence of injection or infiltration can be determined by letting $Q_I = 0$ in equations (8), (9), or (10),

$$x_i = -\frac{(1+\alpha)\alpha}{2q_f}KH_s^2. \tag{11}$$

Once the location of the interface toe is available, one can determine the reduction of the saltwater volume,

$$\Delta V = \int_{y=-\infty}^{y=\infty}\left(\int_{x=0}^{x=x_i} z_i(x)dx - \int_{x=0}^{x=x_t} z_r(x,y)dx\right)dy, \tag{12}$$

in which z_i and z_r represent, respectively, the elevation of the interface without and with the injection well or infiltration pond. Obviously, z_i is a function of x, while z_r is a function of both x and y.

The elevation of the interface above the base can be evaluated by,

$$z = H_s - \frac{1}{1+\alpha}h. \tag{13}$$

In the absence of the aquifer recharge, h is calculated by combining equations (1a) and (3) or (4) and letting $Q_I = 0$,

$$h = \sqrt{-\frac{2(1+\alpha)q_f x}{\alpha K}}. \tag{14}$$

Therefore, z_i can be determined by inserting equation (14) into (13),

$$z_i = H_s - \sqrt{-\frac{2q_f x}{\alpha(1+\alpha)K}}. \tag{15}$$

Inserting equation (15) into equation (12) yields,

$$\Delta V=\int_{y=-\infty}^{y=\infty}\left(-\alpha(1+\alpha)\frac{KH_s^3}{6q_f}-\int_{x=0}^{x=x_t}z_r(x,y)dx\right)dy. \tag{16}$$

Under the condition of well injection or pond infiltration, h is determined respectively by combining equations (1a) and (3), and (1a) and (4),

$$\text{Well injection}: h=\sqrt{\frac{2(1+\alpha)}{\alpha K}\left[-q_f x+\frac{Q_I}{4\pi}\ln\left[\frac{(x+L_I)^2+y^2}{(x-L_I)^2+y^2}\right]\right]}, \tag{17}$$

$$\text{Elliptic pond infiltration}: h=\sqrt{\frac{2(1+\alpha)}{\alpha K}[-q_f x-G+\Re(\Omega_2)]}. \tag{18}$$

Note that the expression for the circular pond infiltration is the same as that of well injection (namely equation (17)) beyond the area below the pond. Similarly, z_r can be derived by inserting equations (17) and (18) into equation (13), respectively, for well injection and elliptic pond injection,

$$\text{Well injection}: z_r=H_s-\sqrt{\frac{2}{(1+\alpha)\alpha K}\left[-q_f x+\frac{Q_I}{4\pi}\ln\left[\frac{(x+L_I)^2+y^2}{(x-L_I)^2+y^2}\right]\right]}, \tag{19}$$

$$\text{Elliptic pond infiltration}: z_r=H_s-\sqrt{\frac{2}{(1+\alpha)\alpha K}[-q_f x+G-\Re(\Omega_2)]}. \tag{20}$$

Then, the reduction in the saltwater volume can be calculated numerically based on equation (16).

3.2. Maximum Net Extraction Rate of the Second Scenario Group

Theoretically, the maximum extraction rate of a single extraction well is obtained when the potentials at the stagnation point (developed by the well) and at the interface tip coincide [*Strack*, 1976]. The maximum extraction rate (Q_E^m) of an extraction well in a flow field with an injection well can be so obtained [*Lu et al*., 2013]. However, for the case with an elliptic infiltration pond, a different method will be employed to achieve Q_E^m due to the difficulty in deriving the locations of the stagnation points analytically, as described below. The maximum net extraction rate (Q_N^m) of an injection-extraction well pair or an infiltration pond-extraction well system is defined as the difference between Q_E^m and a given Q_I.

The discharge potentials for the flow system including a well pair system and a pond-well system are given respectively by,

$$\Phi_W=-q_f x+\frac{Q_I}{4\pi}\ln\left[\frac{(x+L_I)^2+y^2}{(x-L_I)^2+y^2}\right]-\frac{Q_E}{4\pi}\ln\left[\frac{(x+L_E)^2+y^2}{(x-L_E)^2+y^2}\right]+\frac{(1+\alpha)}{2}KH_s^2, \tag{21}$$

$$\Phi_P=-q_f x-G+\Re(\Omega_2)-\frac{Q_E}{4\pi}\ln\left[\frac{(x+L_E)^2+y^2}{(x-L_E)^2+y^2}\right]+\frac{(1+\alpha)}{2}KH_s^2, \tag{22}$$

in which G is expressed in equations (5a) and (5b) in terms of the location, and Ω_2 is complex potentials described in Appendix A. As indicated above, the net extraction rate for the two recharge schemes is represented by $Q_N=Q_E-Q_I$. Similarly, the location of the interface toe can be determined by combining equation (21) or equation (22) with equation (2) and letting $\Phi_W=\Phi_t$ or $\Phi_P=\Phi_t$.

As indicated by *Lu et al*. [2013b], three scenarios with different flow fields can be identified for the well pair system, depending on the values of parameters in equation (21): (1) when the extraction rate is small relative to the injection rate and/or the distance between the two wells is sufficiently large, there is no recirculation zone between the two wells (i.e., no injected water is extracted.); (2) all injected water is extracted, because the extraction rate is significantly large and/or the two wells are close; and (3) part of the injected water is extracted and a partial recirculation zone is formed when intermediate parameter values are adopted. Similar flow field scenarios could occur in the pond-well system.

The stagnation points of the well pair system can be derived, respectively, by letting the first derivatives of equation (21) with respect to x and y equal to zero. The derivation procedure can be found in *Lu et al*.

[2013b]. Note that up to three stagnation points could be developed for the pond-well system. The one with the minimum potential value is considered most critical and is used to derive the maximum net extraction rate using an iteration method. The detailed procedure about how to find the maximum net extraction rate is described by *Lu et al*. [2013b].

The critical condition corresponding to the maximum pumping rate occurs when there is an unstable interface; an infinitesimal increase of the pumping rate would cause the salt water to flow to the inland of the well such that the well can capture it. Therefore, for the pond-well system, the critical condition can be obtained by increasing gradually the pumping rate and comparing the x coordinates of the interface toe with the x coordinate of the well. The critical condition occurs when the x coordinate of a point at the interface toe is first greater than the x coordinate of the well.

3.3. Complex Potential of a Line Infiltration Source

It is of practical interest to compare the performance of an elliptic infiltration pond with a line infiltration source in controlling seawater intrusion, provided that the total recharge rate is the same for the two schemes. The complex potential of the line infiltration source is expressed below [*Strack*, 1989],

$$\Omega_L = \frac{\sigma L}{4\pi}\left\{(Z+1)\ln(Z+1)-(Z-1)\ln(Z-1)+2\ln\left[\frac{1}{2}(z_2-z_1)\right]-2\right\}, \tag{23}$$

where $\sigma[L^2T^{-1}]$ is the infiltration rate, L [L] is the length of the line source, and $Q_I=\sigma L$. z_1 and z_2 are the complex coordinates of the end points of the line source, and Z is the complex variable defined as,

$$Z=\frac{z-\frac{1}{2}(z_1+z_2)}{\frac{1}{2}(z_2-z_1)}, \tag{24}$$

where z is the complex coordinate.

We can determine analytical solutions of the interface toe location under the influence of a single line infiltration source and of the maximum net extraction rate under the line infiltration source-well extraction system, following the method demonstrated above. For comparison, it is assumed that the direction of the line source is the same as that of the major axis of the elliptic pond and the line-source length is equal to the length of the major axis of the elliptic pond.

4. Dimensionless Parameters

To simplify our analysis, the parameters with a unit of length (e.g., x, y, and L) is normalized by H_s and the parameters with a unit of the volumetric flow rate (e.g., Q_I, Q_E, Q_N, and Φ) is normalized by KH_s^2. The dimensionless parameters are denoted by a superscript star. Furthermore, to focus our attention on the impact of well and pond, the values of aquifer parameters are fixed for all cases. The value of q_f^* is assumed to be 0.0008, representing a typical unconfined coastal aquifer [*Werner and Simmons*, 2009]. In the first scenario group, the injection well and the center of the infiltration pond are assumed located at a dimensionless distance $L_I^* = 33.33$ from the coastline. The dimensionless recharge rate (Q_I^*) is assumed to be 0.2667. In practice, the infiltration rate of the pond depends on several design parameters such as the depth of the water table and hydraulic conductivity beneath the pond. Here, the dimensionless infiltration rate (N^*) of the pond in the base case of the first scenario group is assumed to be 0.048, representing a moderate infiltration performance [*Massman*, 2003]. This infiltration rate results in a dimensionless pond area $A^* = 5.56$. The ratio of b to a corresponding to the eccentricity of the ellipse will be varied such that the effect of the pond shape on quantitative indictors can be explored.

In the second scenario group, the injection well (or the center of the infiltration pond) and extraction well are assumed located $L_I^* = 33.33$ and $L_E^* = 53.33$, respectively. The values of N^* and A^* in the base case of the second scenario are kept as in the first scenario. The sensitivity analysis will be conducted for b/a for three different values of N^* and A^*.

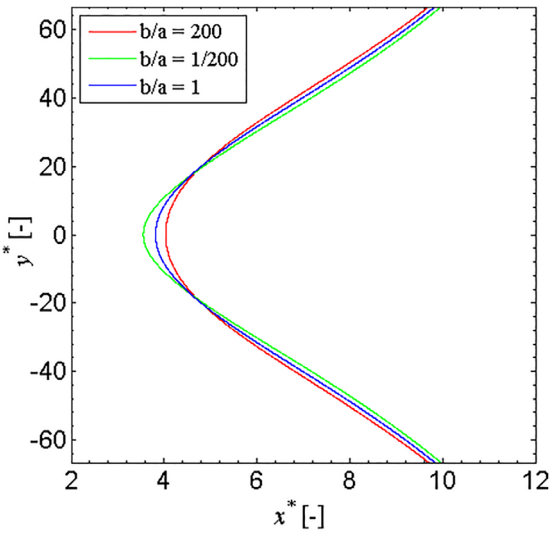

Figure 4. The interface toes developed in cases with $b/a = 200$, 1, and 1/200.

5. Injection Well Versus Infiltration Pond

5.1. Interface Toe Location and Saltwater Volume Reduction

Figure 4 shows the interface toes developed under pond infiltration, where $b/a = 200$ (i.e., major axis is parallel to the coast), 1, and 1/200 (i.e., major axis is perpendicular to the coast), respectively. Since the area of the pond is fixed at $A^* = 5.56$, these ratios of b to a correspond to $a^* = 0.093$, 1.33, and 18.81, and $b^* = 18.81$, 1.33, and 0.093, respectively. The initial interface toe is located at $x_i^* = 16.02$, calculated by equation (11).

Recharge of freshwater into an aquifer leads to the retreat of salt water, with the maximum effect occurring along the x axis. Despite of the significant difference in the shape of the infiltration pond, as shown, the shape of the interface toes developed in these three cases are similar. The dimensionless x coordinates of the three interface toes at $z = 0$ are 3.55, 3.82, and 4.03, respectively, for the cases with $b/a = 200$, 1, and 1/200. The most seaward extent of the interface toe (i.e., at the x axis) occurs in the case with $b/a = 200$, as expected. However, with increasing y, a reversed condition of the interface toe is found for these three cases (i.e., the interface toe in the case with a smaller ratio of b to a is located slightly more seaward).

By calculation, the dimensionless saltwater volume reduction produced by an injection well (or a circular infiltration pond) is 12,963, which is very close to the values obtained for the cases of the two elliptic infiltration ponds with $b/a = 200$ and 1/200 (the relative difference is less than 1%). Obviously, the shape of the infiltration pond has a negligible effect on the saltwater volume reduction for this case.

Furthermore, the comparison between an elliptical infiltration pond and a corresponding line infiltration source indicates that the differences in the interface toe location between the two cases are insignificant (not shown here). Therefore, the quantification of the interface toe under elliptic pond infiltration can be estimated through evaluating the effect of an equivalent line infiltration source, which can simplify the calculation due to the much simpler complex potential expression of the line source.

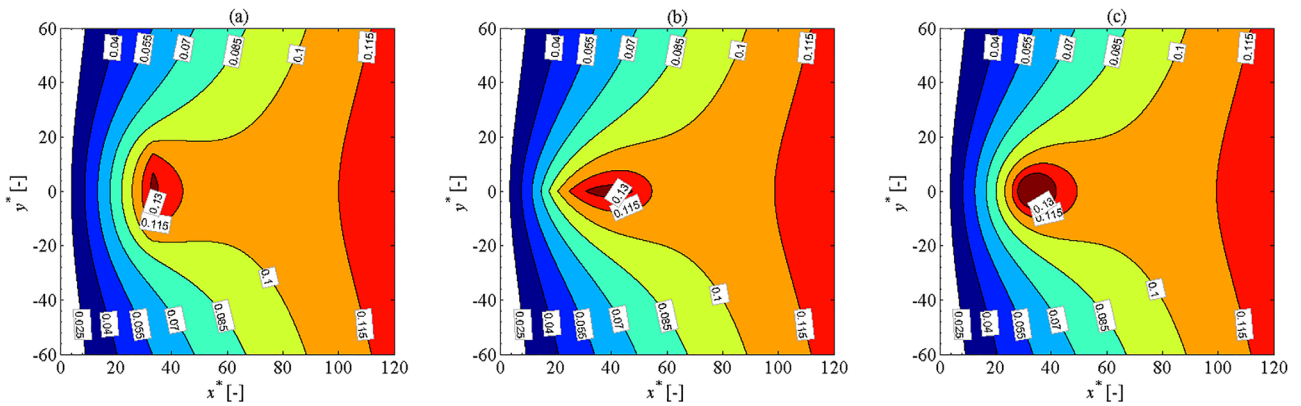

Figure 5. Water table elevations (H_f^*) developed in the freshwater zone (i.e., Zone 2) in cases of (a) $b/a = 200$, (b) b/a = 1/200, and (c) $b/a = 1$.

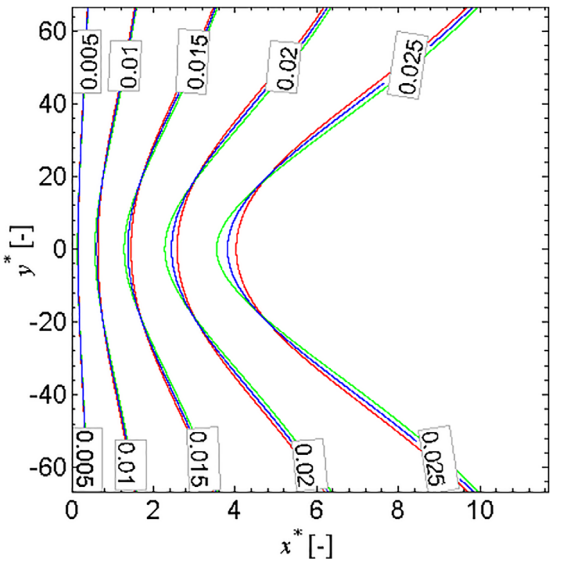

Figure 6. Water table elevations (H_f^*) developed in the saltwater zone (i.e., Zone 1) in cases with $b/a = 200$ (red), 1 (blue), and 1/200 (green).

5.2. Water Table

Figure 5 shows the plan view of piezometric contours (H_f^*) of the freshwater zone (i.e., Zone 2) for the same cases as in Figure 4. It can be proved that the contour line of $H_f^* = 0.025$ coincides with the location of the interface toe. As shown, the differences in the contour line of $H_f^* = 0.025$ among these three cases are very small. However, the significant difference in the shape of the infiltration zone results in a significant difference in the water table within or near the infiltration zone. Taking the contour line $H_f^* = 0.13$ as an example, compressed ellipse-shaped curves are developed in the cases with $b/a = 200$ and 1/200, while an approximately circular curve is found in the case with $b/a = 1$.

Figure 6 shows the plan view of piezometric contours (H_f^*) of the interface zone (i.e., Zone 2) for the same cases as in Figure 4. In comparison with the differences of the piezometric contours of the freshwater zone among three cases, the differences of the water table among these three cases are smaller. Moreover, as shown, the closer the location to the sea, the smaller the differences among these cases.

6. Well Pair Versus Pond-Well System

6.1. Determination of the Maximum Net Extraction Rate

Figure 7 illustrates the method of determining the maximum net extraction rate in the pond-well system, in which $b/a = 200$, $N^* = 0.048$, and $A^* = 5.56$. As shown in Figure 7a, when $Q_E^* = 0.3602$ (i.e., $Q_N^* = 0.09356$), the interface toe is located between the coastline and the extraction well, and as such, the well pumps only freshwater. However, when the extraction rate is slightly increased to $Q_E^* = 0.3603$ (i.e., $Q_N^* = 0.09367$), the interface toe moves abruptly to the inland of the extraction well (Figure 7b). Under this condition, the well pumps salt water and should be abandoned. Therefore, Q_E^{m*} and Q_N^{m*} can be determined as 0.3602 and 0.09356, respectively.

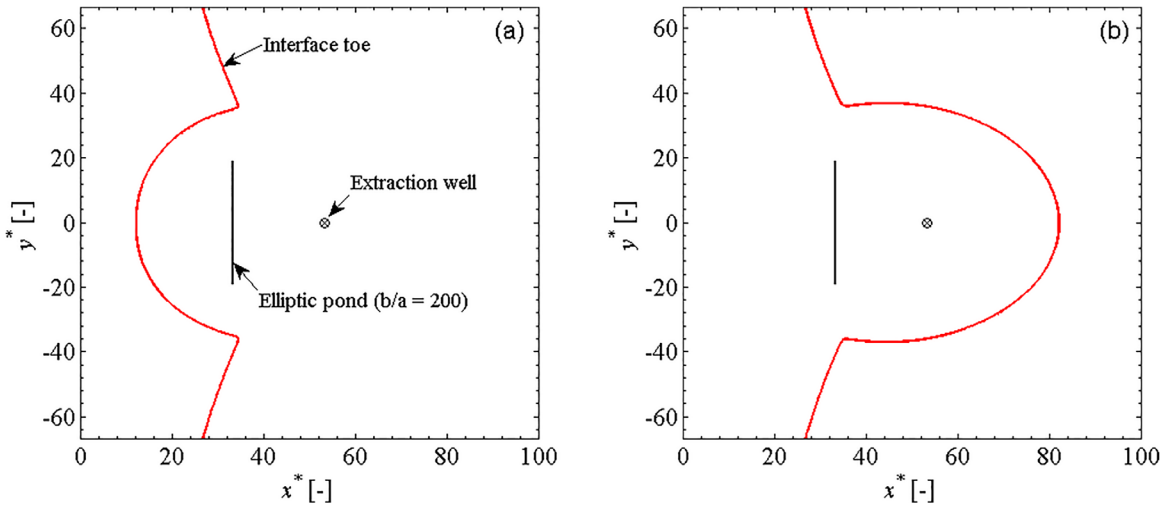

Figure 7. An illustrative example of determining the maximum extraction rate: (a) Q_N^*=0.3602 and (b) Q_N^*=0.3603.

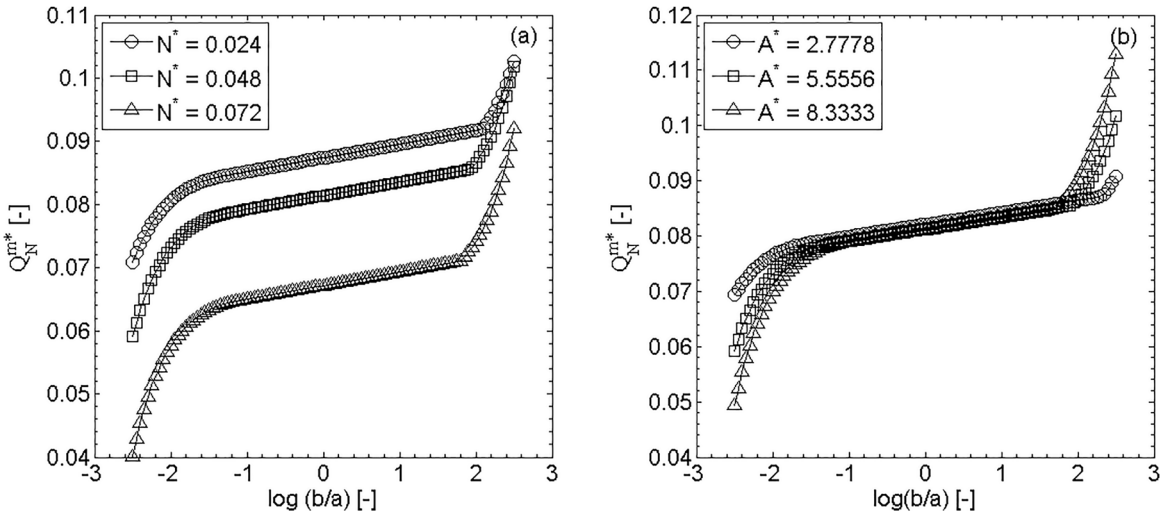

Figure 8. Sensitivity of Q_N^{m*} to b/a for three different values of (a) N^* and (b) A^*.

6.2. Sensitivity Analysis of Q_N^{m*}

Figure 8 shows the sensitivity of Q_N^{m*} to b/a for three different values of $N^* = 0.024$, 0.048, and 0.072, and $A^* = 2.27$, 5.56, and 8.33. As shown, Q_N^{m*} increases with the increasing b/a for all cases. Taking $N^* = 0.024$ and $A^* = 5.56$ as an example, Q_N^{m*} increases from 0.06644 to 0.09356 (an increase of 40%), as b/a increases from 1/200 to 200. Therefore, the pond-well system could significantly outperform the well pair system when a large b/a is chosen. Comparing with the well injection case (i.e., $Q_N^{m*} = 0.08133$ when $a = b$), an increase of 15% in Q_N^{m*} is achieved when $b/a = 200$. Figure 8a indicates that a larger N^* leads to a smaller Q_N^{m*}. However, this conclusion does not hold for a wide range of the recharge rate, as shown in the study of *Lu et al*. [2013b]. Moreover, when b/a is between 1/50 and 200, the sensitivity of Q_N^{m*} to A^* is not significant, as shown in Figure 8b.

Figure 9 shows the comparison of Q_N^{m*} between the pond-well system and line source-well system. It is clearly shown that for a wide range of b/a, the values of Q_N^{m*} are quite close. For an extremely large or small b/a (i.e., the elliptic pond with a large eccentricity), the difference of Q_N^{m*} between the two schemes become significant. For log $(b/a) = 2.5$ (i.e., $b/a = 316$), for example, the values of Q_N^{m*} for the pond-well system and line source-well system are 0.1018 and 0.1089, representing a relative difference of 7%.

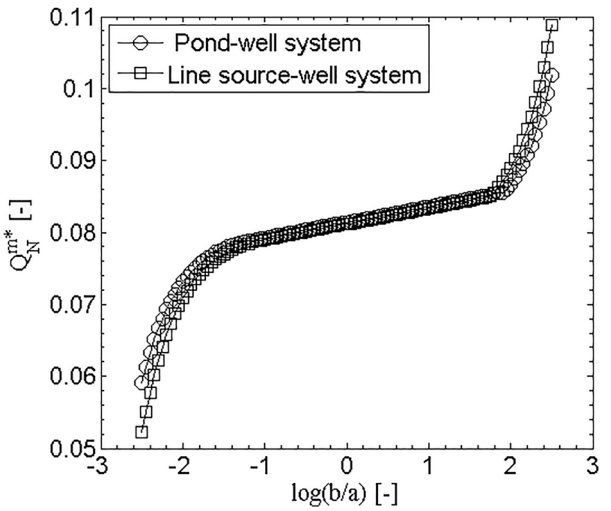

Figure 9. Comparison of Q_N^{m*} between the pond-well system and the line source-well system.

7. Conclusions

We compare the performances of two different types of aquifer recharge schemes (well injection and pond infiltration) in controlling seawater intrusion in an unconfined coastal aquifer using the analytical method based on the potential theory. By exploring two scenario groups, the following conclusions are drawn from the results:

1. The performances of the two aquifer recharge schemes in controlling seawater intrusion are the same, if the infiltration pond is circular and not located above the interface zone, because the resulting analytical solutions of the interface toe for the two cases are the same.
2. The shape of the elliptic infiltration pond has a negligible effect on the

interface toe location as well as the reduction in the saltwater volume for the case of recharge only, despite that a smaller *b/a* results in a larger interface toe retreat.

3. The shape of the elliptic infiltration pond controls the maximum net extraction rate of the pond infiltration-well extraction system. When the major axis of the ellipse is parallel to the coastline, the maximum net extraction rate of the pond-well system could be significantly higher than that of a corresponding well pair system.
4. When evaluating the effect of an elliptic infiltration pond on the interface toe location are similar, a line infiltration source can be used to replace the pond which can simplify the calculation. However, obvious differences in the maximum net extraction rate between the pond-well system and the line source-well system are found for the elliptic pond with a large eccentricity.

Although the study is based on a simple conceptual model that neglects the mixing between freshwater and seawater, aquifer heterogeneity, and transient condition, the results derived are significant, and offer useful initial guidance for practitioners when planning to employ an aquifer recharge strategy to restore a salinized unconfined coastal aquifer.

Appendix A: Expression of the Complex Potential Ω_1 and Ω_2

Stratck [2009] obtained the discharge potential for an elliptical pond using Wirtinger calculus and holomorphic matching. The complex potential Ω_1 is expressed as,

$$\Omega_1 = \frac{Q}{2\pi}\left[\ln\chi + \frac{1}{2}\frac{a-b}{a+b}\frac{1}{\chi^2}\right] \quad \chi\overline{\chi} > 0, \tag{A1}$$

in which χ is given by:

$$\chi = \gamma z + \gamma\sqrt{(z-1)(z+1)}, \tag{A2}$$

where $\gamma = \sqrt{\frac{a-b}{a+b}}$ and $z = \frac{(x-L_I)+iy}{\sqrt{(a^2-b^2)}}$. The expression of Ω_2 is the same as that of Ω_1 except that $z = \frac{(x+L_I)+iy}{\sqrt{(a^2-b^2)}}$. The image Ω_2 is used to maintain a constant potential along the coast.

Acknowledgments
This study was supported by the National Natural Science Foundation of China (51679067), the Fundamental Research Funds for the Central Universities (2015B28714), and the National Key Research Project (2016YFC0402800). We would like to thank Otto D. L. Strack for his helpful discussion and suggestion. The data and Matlab codes used in this paper can be obtained upon request from the corresponding author.

References

Ataie-Ashtiani, B., and H. Ketabchi (2011), Elitist continuous ant colony optimization algorithm for optimal management of coastal aquifers, *Water Resour. Manage.*, *25*, 165–190.
Ataie-Ashtiani, B., A. D. Werner, S. T. Simmons, L. K. Morgan, and C. Lu (2013), How important is the impact of land-surface inundation on seawater intrusion caused by sea-level rise?, *Hydrogeol. J.*, *21*, 1673–1677.
Chang, S. W., and T. P. Clement (2012), Experimental and numerical investigation of saltwater intrusion dynamics in flux-controlled groundwater systems, *Water Resour. Res.*, *48*, W09527, doi:10.1029/2012WR012134.
Cheng, A. H.-D., A. Halhal, D. Naji, and D. Ouazar (2000), Pumping optimization in saltwater-intruded coastal aquifers, *Water Resour. Res.*, *36*, 2155–2165, doi:10.1029/2000WR900149.
Eslamian, S. (2014), *Handbook of Engineering Hydrology*, CRC Press, Boca Raton, Fla.
Herndon, R., and M. Markus (2014), Large-scale aquifer replenishment and seawater intrusion control using recycled water in Southern California, *Bol. Geol. Min.*, *125*(2), 143–155.
Kacimov, A. R., M. M. Sherif, J. S. Perret, and A. Al-Mushikhi (2009), Control of sea-water intrusion by salt-water pumping: Coast of Oman, *Hydrogeol. J.*, *17*, 541–558.
Kaleris, V. K., and A. L. Ziogas (2013), The effect of cutoff walls on saltwater intrusion and groundwater extraction in coastal aquifers, *J. Hydrol.*, *476*, 370–383.
Keuleneer, F. D., and P. Renard (2015), Can shallow open-loop hydrothermal well-doublets help remediate seawater intrusion?, *Hydrogeol. J.*, *23*, 619–629.
Land, M., E. G. Reichard, S. M. Crawford, R. R. Everett, M. W. Newhouse, and C. F. Williams (2004), Ground-water quality of coastal aquifer systems in the West Coast Basin, Los Angeles County, California, 1999–2002, *U.S. Geol. Surv. Sci. Invest. Rep. 2004–5067*, 80 p.
Lee, H. J., and W. R. Normark (2009), *Earth Science in the Urban Ocean: The Southern California Continental Borderland*, *Boulder, Colorado*, Geol. Soc. of Am., Boulder, Colo.
Lu, C., and A. D. Werner (2013), Timescales of seawater intrusion and retreat, *Adv. Water Resour.*, *59*, 39–51.
Lu, C., R. Gong, and J. Luo (2009), Analysis of stagnation points for a pumping well in recharge areas, *J. Hydrol.*, *373*, 442–452.
Lu, C., A. D. Werner, and C. T. Simmons (2013a), Threats to coastal aquifers, *Nat. Clim. Change*, *3*, 605.
Lu, C., A. D. Werner, C. T. Simmons, N. I. Robinson, and J. Luo (2013b), Maximizing net extraction using an injection-extraction well pair in a coastal aquifer, *Ground Water*, *51*, 219–228.
Lu, C., P. Xin, L. Li, and J. Luo (2015), Seawater intrusion in response to sea-level rise in a coastal aquifer with a general-head inland boundary, *J. Hydrol.*, *522*, 135–140.
Luyun, R., K. Momii, and K. Nakagawa (2009), Laboratory-scale saltwater behavior due to subsurface cutoff wall, *J. Hydrol.*, *377*(3–4), 227–236.
Luyun, R., K. Momii, and K. Nakagawa (2011), Effects of recharge wells and flow barriers on seawater intrusion, *Ground Water*, *49*, 239–249.

Mahesha, A. (1996), Control of seawater intrusion through injection-extraction well system, *J. Irrig. Drain Eng.*, *122*, 314–317.
Mahesha, A. (2001), Effect of strip recharge on sea water intrusion in to aquifers, *Hydrol. Sci. J.*, *46*(2), 199–210.
Mantoglou, A. (2003), Pumping management of coastal aquifers using analytical models of saltwater intrusion, *Water Resour. Res.*, *39*(12), 1335, doi:10.1029/2002WR001891.
Masciopinto, C. (2013), Management of aquifer recharge in Lebanon by removing seawater intrusion from coastal aquifers, *J. Environ. Manage.*, *130*, 306–312.
Massman, J. W. (2003), A design manual for sizing infiltration ponds, final research report, *Res. Proj. Agreement Y8265*, Wash. State Transp. Comm., U.S. Dep. of Transp., Tacoma.
Pool, M., and J. Carrera (2010), Dynamics of negative hydraulic barriers to prevent seawater intrusion, *Hydrogeol. J.*, *18*, 95–105.
Raicy, M. C., S. P. Renganayaki, K. Brindha, and L. Elango (2012), Mitigation of seawater intrusion by managed aquifer recharge, in *Managed Aquifer Re-Charge: Methods, Hydrogeological Requirements, Post and Pre-Treatment Systems*, edited by L. Elango, V. C. Goyal, and T. Wintgens, pp. 70–81, Dep. of Geol., Anna Univ., Chennai, India.
Rao, S. V. N., V. Sreenivasulu, S. M. Bhallamudi, B. S. Thandabeswara, and K. P. Sudheer (2004), Planning groundwater development in coastal aquifers, *Hydrol. Sci. J.*, *49*(1), 155–170.
Saeed, M. M., M. Bruen, and M. N. Asghar (2002), A review of modeling approaches to simulate saline-upconing under skimming wells, *Nord. Hydrol.*, *3*, 165–188.
Sheahan, N. T. (1977), Injection/extraction well system—A unique seawater intrusion barrier, *Groundwater*, *15*(1), 32–50.
Sherif, M. M., and K. I. Hamza (2001), Mitigation of seawater intrusion by pumping brackish water, *Transp. Porous Media*, *43*, 29–44.
Shi, L., and J. J. Jiao (2014), Seawater intrusion and coastal aquifer management in China: A review, *Environ. Earth Sci.*, *72*, 2811–2819.
Strack, O. D. L. (1976), A single-potential solution for regional interface problems in coastal aquifers, *Water Resour. Res.*, *12*, 1165–1174.
Strack, O. D. L. (1989), *Goundwater Mechanics*, Prentice-Hall.
Strack, O. D. L. (2009), Using Wirtinger calculus and holomorphic matching to obtain the discharge potential for an elliptical pond, *Water Resour. Res.*, *45*, W01409, doi:10.1029/2008WR007128.
Strack, O. D. L., L. Stoekl, K. Damm, G. Houben, B. K. Ausk, and W. J. de Lange (2016), Reduction of saltwater intrusion by aquifer modification, *Water Resour. Res.*, *52*, 6978–6988, doi:10.1002/2016WR019037.
Sugio, S., K. Nakada, and D. K. Urish (1987), Subsurface seawater intrusion barrier analysis, *J. Hydraul. Eng.*, *113*, 767–779.
Sun, D. M., and S. Semprich (2013), Using compressed air injection to control seawater intrusion in a confined coastal aquifer, *Transp. Porous Media*, *100*(2), 259–278.
Todd, D. (1980), *Groundwater Hydrology*, chap. 14, John Wiley, Chichester, U. K.
Verruijt, A. (1969), An interface problem with a source and a sink in the heavy fluid, *J. Hydrol.*, *8*(2), 197–206.
Werner, A. D. (2010), A review of seawater intrusion and its management in Australia, *Hydrogeol. J.*, *18*, 281–285.
Werner, A. D., and C. T. Simmons (2009), Impact of sea-level rise on seawater intrusion in coastal aquifers, *Ground Water*, *47*, 197–204.
Werner, A. D., J. D. Ward, L. K. Morgan, C. T. Simmons, N. I. Robinson, and M. D. Teubner (2012), Vulnerability indicators of sea water intrusion, *Ground Water*, *50*(1), 48–58.
Werner, A. D., M. Bakker, E. V. A. Post, A. Vandenbohede, C. Lu, B. Ataie-Ashtiani, C. T. Simmons, and D. A. Barry (2013), Seawater intrusion processes, investigation and management: Recent advances and future challenges, *Adv. Water Resour.*, *51*, 3–26.